

Are your MRI contrast agents cost-effective?

Learn more about generic Gadolinium-Based Contrast Agents.



AJNR

Time-of-Flight MR Angiography Targeted to Coiled Intracranial Aneurysms Is More Sensitive to Residual Flow than Is Digital Subtraction Angiography

Naoaki Yamada, Katsuhiko Hayashi, Kenichi Murao, Masahiro Higashi and Koji Iihara

This information is current as of April 17, 2024.

AJNR Am J Neuroradiol 2004, 25 (7) 1154-1157
<http://www.ajnr.org/content/25/7/1154>

Time-of-Flight MR Angiography Targeted to Coiled Intracranial Aneurysms Is More Sensitive to Residual Flow than Is Digital Subtraction Angiography

Naoaki Yamada, Katsuhiko Hayashi, Kenichi Murao, Masahiro Higashi, and Koji Iihara

BACKGROUND AND PURPOSE: For intracranial aneurysms treated with Guglielmi detachable coils, long-term follow-up is mandatory because coil compaction may occur and aneurysms may recur. The purpose of this study was to establish a noninvasive technique to visualize residual flow in coiled aneurysms.

METHODS: We designed a 3D time-of-flight (3D-TOF) MR angiography (MRA) technique targeted to depict coiled aneurysms that employed a very short TE (1.54–1.60 ms) and a high spatial resolution ($0.3 \times 0.3 \times 0.3 \text{ mm}^3$ with zero-filling) to diminish spin dephasing. To diminish spin saturation, image volume was carefully positioned so that the neck of the targeted aneurysm was within 2 cm of the inflow portion along the stream of blood. Fifty-one MRA images of 39 coiled aneurysms in 39 patients were compared with digital subtraction angiography (DSA) images. DSA and MRA findings were interpolated retrospectively for parent and branch arteries' patency, as well as residual flow in aneurysms. In the latest 11 MR studies, a dark-blood 3D turbo spin-echo sequence was added to MRA to negate the effect high-signal-intensity thrombus.

RESULTS: MRA visualized all parent and branch arteries with DSA confirmation. MRA visualized residual flow more frequently (38 studies) than did DSA (25 studies). Residual flow space visualized with MRA was always similar to or larger than that with DSA. The dark-blood sequence completely suppressed intraluminal high signal intensity on MRA images and confirmed that the high signal intensity was not due to thrombus.

CONCLUSION: TOF MRA targeted to depict coiled intracranial aneurysms is noninvasive and superior to DSA in visualization of residual flow and, hence, useful for follow-up of coiled aneurysms.

Endovascular treatment of intracranial aneurysms with Guglielmi detachable coils has become widely performed worldwide as a less invasive alternative to surgical clip placement. The outcome 1 year after treatment of ruptured aneurysms was better with endovascular coil placement than with neurosurgical clip placement, but the issue of long-term efficacy has not been resolved (1). It is generally agreed that long-term angiographic follow-up monitoring is man-

datory for coiled aneurysms, because coil compaction may occur and aneurysms may recur (2, 3).

As a follow-up technique, digital subtraction angiography (DSA), the current standard technique, is invasive and carries some risks of cerebrovascular accident. On the other hand, MR angiography (MRA) is safe and noninvasive. At present, however, MRA without (4, 5) or with (6) use of contrast material is less sensitive to residual flow than is DSA.

Spin dephasing and saturation are two severe limitations in 3D time-of-flight (3D-TOF) MRA. Diminution of signal intensity loss due to dephasing will be resolved most effectively with implementation of very short TE (7). Recent development of technology permitted us to use a much shorter TE with a sufficient spatial resolution. We considered that the second problem—the saturation of inflowing spins causing progressive signal intensity loss toward outflow portions of the imaged volume—will be resolved if an

Received October 25, 2003; accepted after revision January 5, 2004.

From the Department of Radiology and Nuclear Medicine (N.Y., M.H.), and Neurosurgery (K.H., K.M., K.I.), National Cardiovascular Center, Osaka, Japan.

Address correspondence to Naoaki Yamada, MD, Department of Radiology and Nuclear Medicine, National Cardiovascular Center, 5-7-1, Fujishiro-dai, Suita, Osaka, 565-8565 Japan.

© American Society of Neuroradiology

aneurysm is placed near the inflow portion of the imaged volume.

Methods

From February 2002 to October 2003, we performed MRA of coiled intracranial aneurysms for long-term follow-up or as a baseline for follow-up after coil placement in patients who gave informed consent. MRA as a baseline was scheduled in an early period after coil placement and in a period around follow-up DSA in the chronic phase. Seventy patients with 70 coiled aneurysms uneventfully and successfully underwent 98 MRA studies. Included in this study were MRA images obtained within 3 days after coil placement (early phase, $n = 24$), and MRA within 7 days of follow-up DSA 5–41 (9 ± 7) months after coil placement (chronic phase, $n = 27$). Consequently, 51 MRA studies of 39 coiled aneurysms (two ruptured) of 39 patients were compared with the corresponding DSA studies. The mean age \pm SD of the patients was 59 years \pm 9; nine patients were male. Aneurysms were located in internal carotid artery ($n = 27$), anterior cerebral artery ($n = 1$), basilar artery ($n = 10$), and vertebral artery ($n = 1$). Maximum aneurysmal diameter ranged from 3 to 22 mm ($7.1 \text{ mm} \pm 3.7$).

MRA was performed by radiologists (N.Y., M.H.) by using a standard head coil on a clinical machine operating at 1.5 T with a high-performance gradient coil (Magnetom Sonata; Siemens, Erlangen, Germany). We designed an MRA sequence targeted to coiled aneurysms by using a noncontrast 3D-TOF MRA technique. To diminish the spin saturation, imaged volume was carefully positioned so that the neck of the targeted aneurysm was within 2 cm of the inflow portion along the stream of blood. Positioning was done with multiple sagittal scout images of 2D-TOF MRA. To diminish the spin dephasing, a very short TE (1.54–1.60 ms) with a high spatial resolution (voxel size: $0.3 \times 0.3 \times 0.3 \text{ mm}$ with zero-filling) was employed. Other imaging variables were TR, 35 ms; flip-angle, 25°; in-plane matrix, 256 (512 with zero-filling); field of view, 15 cm; partition, 120 with zero-filling; and the acquisition time, 11 minutes. Flow compensation and variable flip-angle excitation techniques were not employed.

MRA was processed with maximum intensity projection (MIP) closely targeted to a coiled aneurysm. MIP was reconstructed in many orientations around at least two axes. In the best MIP projection, in which residual flow was most widely visualized, depth and width of the neck remnant were measured by using a caliper. Source and multiplanar reconstruction

Correlation between MRA and DSA findings

		MRA		
		CO	RF	Total
DSA	co	13	13 (1)	26 (1)
	rf	0	25 (1)	25 (1)
Total		13	38 (2)	51 (2)

Note.—co, complete obliteration; rf, residual flow (includes neck remnant and body filling). Numbers in parentheses indicates body filling.

(MPR) images were used to observe location of residual flow in aneurysms.

DSA was performed by neurosurgeons (K.H., K.M.) by using a standard biplane angiographic system with rotational 3D-DSA. For determination of residual flow, DSA images were obtained in anteroposterior, lateral, and the working views (oblique view is optimal for neck observation). The working view was determined on the basis of preoperative examination that included 3D-DSA findings.

DSA and MRA were interpreted for patency of the parent artery and branch artery adjacent to the coiled aneurysms, as well as for presence of residual flow in coiled aneurysms. Residual flow was categorized as neck remnant (flow at the neck or around the coil mesh that is continuous from the neck), body filling (flow in the coil mesh), and complete obliteration.

In the last 11 of 51 MR studies, dark-blood imaging was added to the MRA sequences by using the 3D turbo spin-echo technique with spatial presaturation to suppress inflowing spins. Spatial resolution was the same as that of MRA (voxel size, $0.3 \times 0.3 \times 0.3 \text{ mm}$ with zero-filling). Other imaging parameters were TR, 700 ms; TE, 12 ms; partition, 24; and acquisition time, 9 minutes. Imaged volume was placed at the neck of aneurysms.

DSA findings were interpreted from a hardcopy by a neurosurgeon (K.H.) who was blinded to MRA findings. MRA was interpreted on a console of the MR system by a radiologist (N.Y.) who was unaware of DSA interpretation. In MRA interpretation, DSA was used to observe the preoperative location of aneurysm and shape of parent and branch arteries. Both interpreters assessed all aneurysms with residual flow to compare the extent of residual flow shown by MRA versus that shown by DSA; findings were determined by means of consensus. Statistical analysis was done by an author (N.Y.).

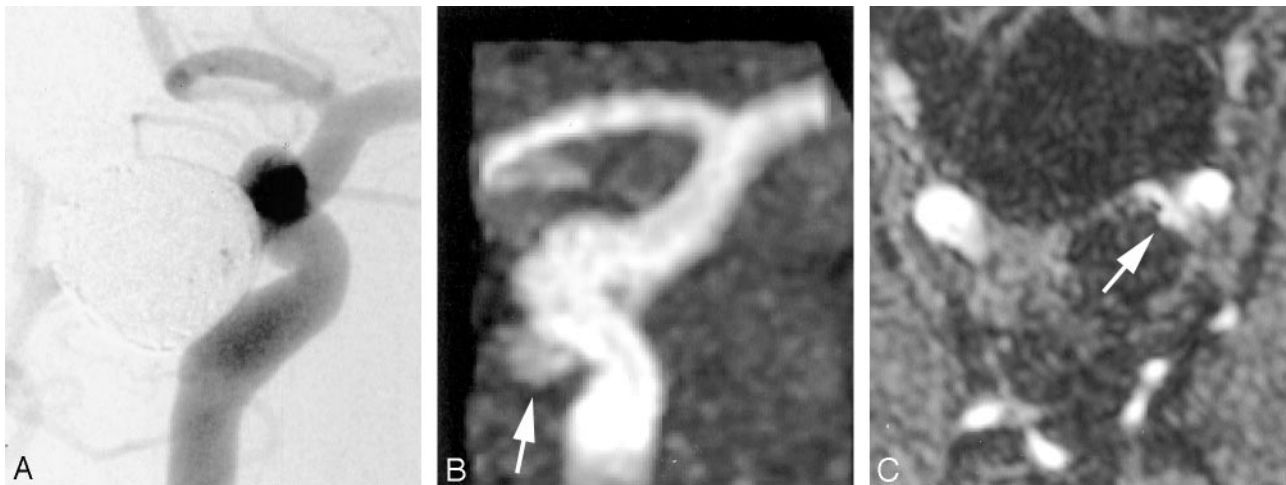


FIG 1. A thin-neck remnant invisible with initial DSA.

A, Oblique DSA image at the end of coil placement shows no flow in the aneurysm at left internal carotid artery (complete obliteration). B and C, MRA images 3 days after coil placement. Closely targeted MIP to the aneurysm in a projection similar to that of the DSA (B) and MRA source image (C) show a neck remnant that is thin and relatively deep (arrows).

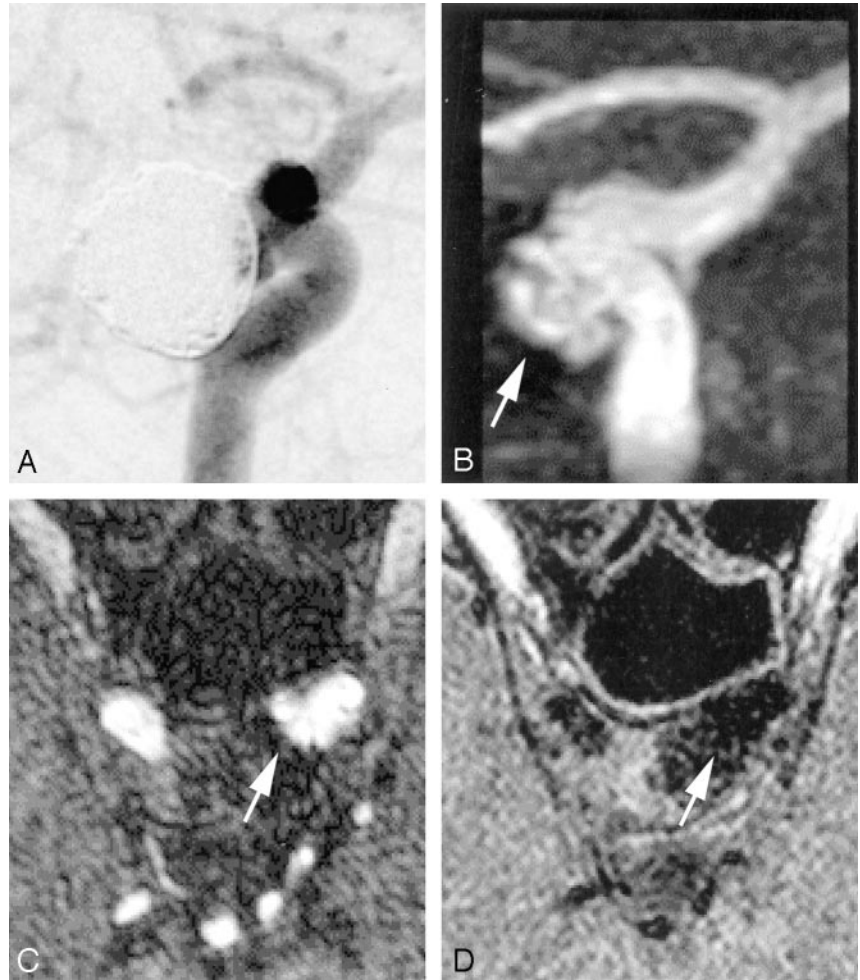


FIG 2. A thick-neck remnant visualized with follow-up DSA images obtained 8 months after initial images.

A, DSA image shows a neck remnant.

B and C, Closely targeted MIP (B) and source image (C) of MRA show a neck remnant (arrows) that is thick and larger than that visualized with DSA.

D, Black-blood image obtained by using 3D turbo spin-echo shows no signal intensity in the aneurysm (arrow) and arteries.

Results

MRA showed all 25 residual flows (24 neck remnants and one body filling) that were visualized with DSA. In addition, MRA showed 13 residual flows (12 neck remnants and one body filling) in 26 complete

obliterations seen with DSA (Table). The McNemar test that is a χ^2 test for paired sample revealed significant difference between MRA and DSA ($P = .0009$). Thin-neck remnants had a tendency to be invisible with DSA (Fig 1). Width of neck remnants



FIG 3. Signal intensity void in parent artery and susceptibility artifact immediately after coil placement.

A, DSA shows an aneurysm at basilar artery-superior cerebellar artery bifurcation at the end of coil placement. Neck remnant (arrowhead) and protrusion of a coil into the basilar artery (arrow) are observed.

B, Targeted MIP of MRA image obtained 3 days after coil placement shows neck remnant more clearly than does DSA image (arrowhead). Signal intensity loss in the basilar artery (arrow) is due to coil protrusion. Signal intensity loss in left posterior cerebral artery (asterisk) is due to susceptibility artifact of the clip in another aneurysm at the left internal carotid-posterior communicating artery bifurcation.

on MRA images was $1.7 \text{ mm} \pm 0.7$ in the 12 neck remnants invisible with DSA, which was significantly smaller than the width ($3.1 \text{ mm} \pm 0.9$) in the 23 DSA visible remnants ($P = .006$, two-tailed Mann-Whitney U test). On the other hand, depth of neck remnants showed no significant difference between DSA invisible neck remnants ($1.7 \text{ mm} \pm 1.4$) and visible neck remnants ($2.0 \text{ mm} \pm 1.0$). Residual flow space visualized with MRA was always similar to or larger than that with DSA (Figs 1–3).

The dark-blood sequence completely suppressed high signal intensity on MRA images (Fig 2) for all 11 MR studies, which included seven studies with residual flow (four early phase, three chronic phase). It was confirmed that high signal intensity on MRA images was due to inflow spin, not thrombus.

MRA successfully depicted all parent and adjacent arteries of coiled aneurysms. Localized signal intensity loss in the parent artery that mimicked stenosis was observed in four aneurysms in which DSA showed coil protrusion into the parent artery (Fig 3).

Discussion

On the basis of the results of this study, we have replaced DSA with MRA for long-term follow-up of coiled aneurysms. As compared with previous studies, we used a shorter TE and a higher spatial resolution to diminish spin dephasing. In addition, we made use of inflow phenomena to enhance blood signal. Inflowing spin is the most powerful enhancer of blood signal, because it has full magnetization if the observation point is placed close to the inflow portion, whereas gadolinium recovers magnetization only partially with a short TR. Owing to the opacity of coils in the setting of conventional radiographs and the limited number of DSA projections, DSA was less sensitive to residual flow than was MRA, particularly in thin remnants.

3D-DSA was not used for evaluation of residual flow, because it is artificial and the boundary between coil mass and residual flow is unclear. We have several years of experience with 3D-DSA and recently stopped using it to treat coiled aneurysms; however, if we refer to source images of 3D-DSA, visibility of residual flow by DSA might improve the results of this study.

Acute and subacute thrombus or hematoma may have high signal intensity on T1-weighted images (8). Because TOF MRA is a T1-weighted imaging technique for static tissue, thrombus or hematoma can have high signal intensity. In the series of Derdeyn et al (5), artifact and hemorrhage mimicked residual flow in two of 18 MR studies. Brunereau et al (4), however, did not observe this artifact in their 27 MR studies. We also did not observe high signal intensity that was likely to be thrombus or artifact. If a high-signal-intensity thrombus is suspected on the basis of MRA findings, we can use the dark-blood sequence to confirm it or rule it out. Although the number of coiled aneurysms confirmed not to have high-signal-intensity thrombus is small in this study group ($n = 11$), we continue to accumulate data. Through the end of November 2003, more than 30

MRA studies were performed with dark-blood imaging, and no thrombus with high signal intensity was observed in coiled aneurysms.

The time needed to perform MRA is short: 20 minutes, including scout imaging and positioning of MRA and 30 minutes if dark-blood imaging is added. Processing of MRA (MIP or MPR) is simple and available with most MR systems. Our MRA technique may be limited to high-end systems, because very short TEs with high spatial resolution are available by using high-performance gradient coils.

There are a few minor limitations to MRA. If a patient has another coiled aneurysm at a different position, another MRA study is necessary, because spin saturates as it travels a long distance in an imaged volume. MRA cannot depict the coils themselves and cannot determine whether an increase of neck remnant is due to coil compaction or regrowth of aneurysm. Coil compaction, however, can be estimated by using conventional radiographs. Localized signal intensity loss in the parent artery does not indicate stenosis, because protrusion of the coils induces turbulence and spin dephasing. Aneurysms adjacent to surgical clips may not be estimated by MRA findings owing to the susceptibility artifact (spin dephasing due to magnetic field inhomogeneity).

Conclusion

We presented a TOF MRA technique targeted to coiled intracranial aneurysms with a very short TE, high spatial resolution, and positioning of aneurysm neck close to inflow portion. MRA is noninvasive and superior to DSA in visualization of residual flow in aneurysms, and therefore, is useful for follow-up of coiled aneurysms. Long-term follow-up by using MRA is undergoing at our hospital and may provide a solution for the issue of final outcome of coil embolization.

References

1. Molyneux A, Kerr R, Stratton I, et al. **International Subarachnoid Aneurysm Trial (ISAT) of neurosurgical clipping versus endovascular coiling in 2143 patients with ruptured intracranial aneurysms: a randomised trial.** *Lancet* 2002;360:1267–1274
2. Thornton J, Debrun GM, Aletich VA, et al. **Follow-up angiography of intracranial aneurysms treated with endovascular placement of Guglielmi detachable coils.** *Neurosurgery* 2002;50:239–249; discussion 249–250
3. Murayama Y, Nien YL, Duckwiler G, et al. **Guglielmi detachable coil embolization of cerebral aneurysms: 11 years' experience.** *J Neurosurg* 2003;98:959–966
4. Brunereau L, Cottier JP, Sonier CB, et al. **Prospective evaluation of time-of-flight MR angiography in the follow-up of intracranial saccular aneurysms treated with Guglielmi detachable coils.** *J Comput Assist Tomogr* 1999;23:216–223
5. Derdeyn CP, Graves VB, Turski PA, et al. **MR angiography of saccular aneurysms after treatment with Guglielmi detachable coils: preliminary experience.** *AJNR Am J Neuroradiol* 1997;18:279–286
6. Boulin A, Pierot L. **Follow-up of intracranial aneurysms treated with detachable coils: comparison of gadolinium-enhanced 3D time-of-flight MR angiography and digital subtraction angiography.** *Radiology* 2001;219:108–113
7. Schmalbrock P, Yuan C, Chakeres DW, et al. **Volume MR angiography: methods to achieve very short echo times.** *Radiology* 1990;175:861–865
8. Moody AR, Pollock JG, O'Connor AR, Bagnall M. **Lower-limb deep venous thrombosis: direct MR imaging of the thrombus.** *Radiology* 1998;209:349–355